The EMBO Journal (2011) 30, 4185–4197 | © 2011 European Molecular Biology Organization | Some Rights Reserved 0261-4189/11
www.embojournal.org

THE EMBO JOURNAL

EMBO open

Structural analysis of the Ras-like G protein MglA and its cognate GAP MglB and implications for bacterial polarity

Mandy Miertzschke[1], Carolin Koerner[1], Ingrid R Vetter[2], Daniela Keilberg[3], Edina Hot[3], Simone Leonardy[3,4], Lotte Søgaard-Andersen[3] and Alfred Wittinghofer[1,*]

[1]Structural Biology Group, Max-Planck-Institute for Molecular Physiology, Dortmund, Germany, [2]Department of Physical Biochemistry, Max-Planck-Institute for Molecular Physiology, Dortmund, Germany and [3]Department of Ecophysiology, Max-Planck-Institute for Terrestrial Microbiology, Marburg, Germany

The bacterium *Myxococcus xanthus* uses a G protein cycle to dynamically regulate the leading/lagging pole polarity axis. The G protein MglA is regulated by its GTPase-activating protein (GAP) MglB, thus resembling Ras family proteins. Here, we show structurally and biochemically that MglA undergoes a dramatic, GDP–GTP-dependent conformational change involving a screw-type forward movement of the central β2-strand, never observed in any other G protein. This movement and complex formation with MglB repositions the conserved residues Arg53 and Gln82 into the active site. Residues required for catalysis are thus not provided by the GAP MglB, but by MglA itself. MglB is a Roadblock/LC7 protein and functions as a dimer to stimulate GTP hydrolysis in a 2:1 complex with MglA. *In vivo* analyses demonstrate that hydrolysis mutants abrogate *Myxococcus*' ability to regulate its polarity axis changing the reversal behaviour from stochastic to oscillatory and that both MglA GTPase activity and MglB GAP catalysis are essential for maintaining a proper polarity axis.

The EMBO Journal (2011) **30,** 4185–4197. doi:10.1038/emboj.2011.291; Published online 16 August 2011
Subject Categories: signal transduction; structural biology
Keywords: bacterial Ras-like G protein; cell polarity; GTPase-activating protein; intrinsic arginine finger; Roadblock/LC7 domain

Introduction

Small G proteins of the Ras superfamily can be divided into five major subfamilies: Ras, Rho, Rab, Arf/Arl and Ran. By cycling between an inactive, GDP-bound and an active, GTP-bound conformation, they act as nucleotide-dependent molecular switches regulating cellular functions including growth, polarity and differentiation (Vetter and Wittinghofer, 2001; Cox and Der, 2010). In the active GTP-bound conformation, they interact with effectors to elicit a downstream response (Wittinghofer and Nassar, 1996; Herrmann, 2003). Since the intrinsic rates of GTP hydrolysis and GDP/GTP exchange are very slow, their cycle is regulated by GTPase-activating proteins (GAPs) and guanine nucleotide exchange factors (GEFs), which increase the intrinsic rates by orders of magnitude (Bos *et al*, 2007).

GAPs stimulate GTP hydrolysis by complementing and/or stabilizing the G protein catalytic site in the transition state. GTPase activation relies on correct positioning of a nucleophilic water molecule by a crucial glutamine (for Ras, Rho, Ran, Rab, Arf/Arl) or histidine (Sar, elongation factors) (Scheffzek and Ahmadian, 2005; Bos *et al*, 2007). Rho-, Ras-, Rab-, Arf- and Arl-specific GAPs supply an arginine finger *in trans*, which stabilizes the catalytic glutamine of the G protein and neutralizes the negative charge developing in the transition state (Scheffzek and Ahmadian, 2005; Bos *et al*, 2007). Rap (Daumke *et al*, 2004; Scrima *et al*, 2008) and RheB (Inoki *et al*, 2003; Tee *et al*, 2003) specific GAPs complement the active site of the G protein by inserting a so-called asparagine thumb. Gα subunits of heterotrimeric G proteins contain the glutamine as well as an intrinsic arginine and stimulation by RGS proteins occurs by stabilization of the intrinsic catalytic machinery (Sprang, 1997; Sprang *et al*, 2007).

The annotation of many bacterial genomes indicated the presence of a number of small G proteins (Brown, 2005), such as Era (Ahnn *et al*, 1986) and EngA (Mehr *et al*, 2000). Most are thought to be involved in aspects of ribosome biogenesis and/or function (Brown, 2005). Clear mechanistically defined GEFs or GAPs have not yet been reported for these (Wittinghofer and Vetter, 2010) except the *Escherichia coli* GTPase Der that is stimulated indirectly by the GAP-like protein Yih1 (Hwang and Inouye, 2010). Moreover, many pathogenic bacteria have evolved virulence factors (effectors) that are injected into eukaryotic cells to manipulate the function of host G proteins of the Ras superfamily either by covalent modification or by acting as highly active GAPs or GEFs (Alto, 2008): *Salmonella* spp. proteins SopE and SopE2 are GEFs for Rac and Cdc42, while *Legionella pneumophila* proteins RalF and DrrA/SidA are GEFs for Arf and Rab1, respectively. Other effector proteins such as *Yersinia* spp. YopE, *Salmonella* spp. SptB, *Pseudomonas aeruginosa* ExoS and *L. pneumophila* LepB are GAPs for Rho and Rab, respectively. These factors are not structurally related to host's GEFs or GAPs but use similar catalytic mechanisms.

Ras-like G proteins have recently been shown to regulate polarity in bacteria (Shapiro *et al*, 2009; Leonardy *et al*, 2010; Zhang *et al*, 2010). The rod-shaped bacterium *Myxococcus*

*Corresponding author. Structural Biology Group, Max-Planck-Institute for Molecular Physiology, Otto-Hahn-Strasse 11, Dortmund D-44227, Germany.
Tel.: +49 231 133 2100; Fax: +49 231 133 2199;
E-mail: alfred.wittinghofer@mpi-dortmund.mpg.de
[4]Present address: Ingenieurbüro Gunter Reimann, Dorfstraße 2A, Wittenberg 06889, Germany

Received: 24 May 2011; accepted: 15 July 2011; published online: 16 August 2011

xanthus provide a simple model system to understand cell polarity. *M. xanthus* cells move in the direction of their long axis by means of two motility systems (Leonardy *et al*, 2008). The S-motility system depends on type IV pili that are assembled at the leading pole (Sun *et al*, 2000) and undergo cycles of extension and retraction (Merz *et al*, 2000; Skerker and Berg, 2001; Clausen *et al*, 2009). The A-motility system depends on focal adhesion complexes assembled at the leading pole and distributed along the cell body (Mignot *et al*, 2007). Occasionally, cells stop and then resume motility in the opposite direction corresponding to an inversion of the leading/lagging pole polarity axis. Reversals are induced by the Frz chemosensory system (Blackhart and Zusman, 1985) and during a reversal, the polarity of the two motility systems is inverted (Leonardy *et al*, 2008). The functionality of both motility systems depends on localization of proteins to the correct cell poles between reversals and their dynamic pole-to-pole relocation during reversals (Mignot *et al*, 2005; Leonardy *et al*, 2007; Bulyha *et al*, 2009).

The Ras-like G protein MglA functions as a nucleotide-dependent molecular switch that regulates the dynamic polarity of motility proteins (Leonardy *et al*, 2010; Patryn *et al*, 2010; Zhang *et al*, 2010). MglA establishes the correct polarity of dynamically localized motility proteins between reversals, and induces their pole-to-pole relocation during reversals (Leonardy *et al*, 2010; Zhang *et al*, 2010). MglA binds guanine nucleotides with nM affinities, and possesses a slow intrinsic GTPase activity. MglB, encoded in an operon with MglA, is the cognate GAP of MglA (Leonardy *et al*, 2010; Zhang *et al*, 2010). Between reversals, MglA·GTP and MglB localize to the leading and lagging pole, respectively, in this way defining the leading/lagging polarity axis. The binding to opposite poles is thought to involve a mutual exclusion mechanism. During reversals, and induced by the Frz system, MglA and MglB undergo pole-to-pole relocation causing an inversion of the leading/lagging polarity axis. Thus, between reversals MglA·GTP and MglB establish a stable leading/lagging polarity axis that is occasionally inverted in response to Frz activity.

MglB possesses a Roadblock/LC7 domain. Although no function has been assigned to this domain, it has been implicated in NTPase regulation (Koonin and Aravind, 2000). Intriguingly, the absence of conserved arginine, asparagine or histidine residues as found in eukaryotic GAPs raised the question of how MglB performs its GAP function. Moreover, the observation that MglB is likely an oligomer added to the complexity of understanding MglB GAP activity.

To further the understanding of how MglA and MglB dynamically regulate polarity *in vivo*, we used crystallographic and biochemical approaches to elucidate the structures of MglA and MglB and their complex. *In vivo* analyses demonstrate that MglA GTPase activity and MglB GAP activity is essential for maintaining a stable leading/lagging polarity axis that is only occasionally inverted.

Results

Structure of the prokaryotic Ras-like G protein MglA

We previously showed that native MglA/B proteins from *M. xanthus* could not be expressed as soluble proteins in *E. coli* and that *Thermus thermophilus* MglA/B proteins can be used as model systems for the *M. xanthus* proteins (Leonardy *et al*, 2010). MglA (22 kDa) contains most of the conserved residues required for guanine nucleotide binding and GTP hydrolysis (Figure 1A). A minor difference is the replacement of aspartate of the consensus DxxGQ/H/T (G4) motif by $_{78}$TxxGQ$_{82}$. A more pronounced alteration of the G domain is an extra long switch I region between α1 and β2 that appears to place MglA closer to the Arf subfamily of the Ras superfamily G proteins.

GDP-bound *T.t.*MglA crystallized in space group P1 (Supplementary Table SI). The asymmetric unit contained two MglA·GDP monomers contacting each other via the C-terminal α5-helix but also forming β-sheet dimers via β2* crystal contacts (Supplementary Figure S1). MglA displays a typical G domain fold with a six-stranded β-sheet surrounded by five α helices (Figure 1B). It has two extra β-strands: β0 at the N-terminus forms a β hairpin with the canonical β1, and β2* precedes and is anti-parallel to β2. An extra β-strand similar to β2* was observed in Ran·GDP where it becomes part of the switch I loop in Ran·GTP (Vetter *et al*, 1999). Although a DALI search supports Ras as being the closest structural homologue, MglA shows structural elements of the Ran and Arf subfamily proteins (Figure 1C) that were not obvious from alignments or secondary structure prediction. This is particularly obvious from the GDP–GTP structural transition (see below).

In the GDP-bound MglA structure, no Mg^{2+} coordinating the α- and/or β-phosphates of GDP was detected. Furthermore, no other residue such as a lysine as in Arl3 (Hillig *et al*, 2000) is found in the canonical position of magnesium. Instead, the main chain nitrogen of Gly81 in switch II does coordinate the β-phosphate of GDP. Apart from the absence of Mg^{2+} and its ligands, the location and conformation of GDP is canonical. Dissociation kinetics using MglA labelled with mGDP or mGppNHp in order to confirm Mg^{2+} dependency of mGDP and mGppNHp release, respectively, showed us that the nucleotide-free protein used in steady-state equilibrium titrations to measure nucleotide affinities as described previously (Leonardy *et al*, 2010) is not stable enough. Earlier observations indicated that association rates of G nucleotides were rather similar in the range of 10^5–$10^6\,M^{-1}\,s^{-1}$ (Rensland *et al*, 1995; Veltel *et al*, 2008b) while from the dissociation kinetics, we find that the dissociation of mant-labelled GDP from MglA is $3\times10^{-4}\,s^{-1}$, indicating a nanomolar affinity, which does not appreciably change in the presence of 10 mM EDTA supporting the notion that GDP binding does not require Mg^{2+}. Dissociation of mGppNHp is much faster, $2.8\times10^{-2}\,s^{-1}$, indicating that the affinity to the triphosphate conformation is not only five-fold as previously reported (Leonardy *et al*, 2010) but even about 100-fold weaker.

Structure of the prokaryotic Roadblock/LC7 protein MglB

MglB has considerable homology to other Roadblock/LC7 proteins such as p14 and MP1 (Figure 2A and C) and acts as the cognate GAP for MglA (Leonardy *et al*, 2010). In proteolysis experiments, we initially identified a fragment comprising residues 6–139 (MglB from now), which was stable and as active as full-length MglB (residues 1–163) in MglA binding and stimulation of MglA GTPase activity (Supplementary Figure S2A and B). We generated numerous crystals of varying space groups of MglB. In crystals that belonged to

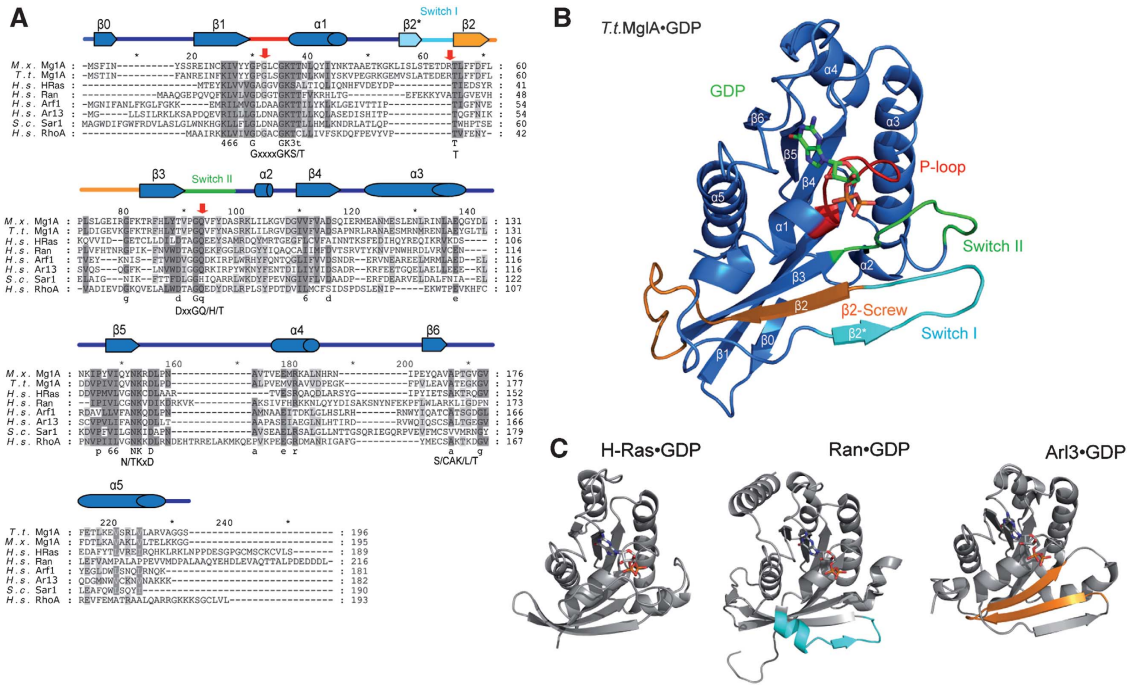

Figure 1 Structure of MglA. (**A**) Alignment of MglA proteins from *M. xanthus* (*M.x.*) and *T. thermophilus* (*T.t.*) to Ras-like G proteins from *Homo sapiens* (*H.s.*) and Sar1 from *Saccharomyces cerivisiae* (*S.c.*). Conserved residues are highlighted in dark and light grey dependent on their degree of conservation. The G1–G5 motifs and switch regions characteristic for the G domain and the secondary structure elements of MglA are shown below and above the alignment, respectively. Red arrows indicate residues mutated for biochemical studies. (**B**) Structure of *T.t.*MglA bound to GDP. Switch I (light blue), switch II (green), P-loop (red) and other characteristic structural elements such as the β2-screw (orange) are indicated. (**C**) Structures of GDP-bound human H-Ras (2cld), Ran (3GJ0) with switch I β-sheet (blue) and Arl3 (1FZQ) with interswitch toggle (orange).

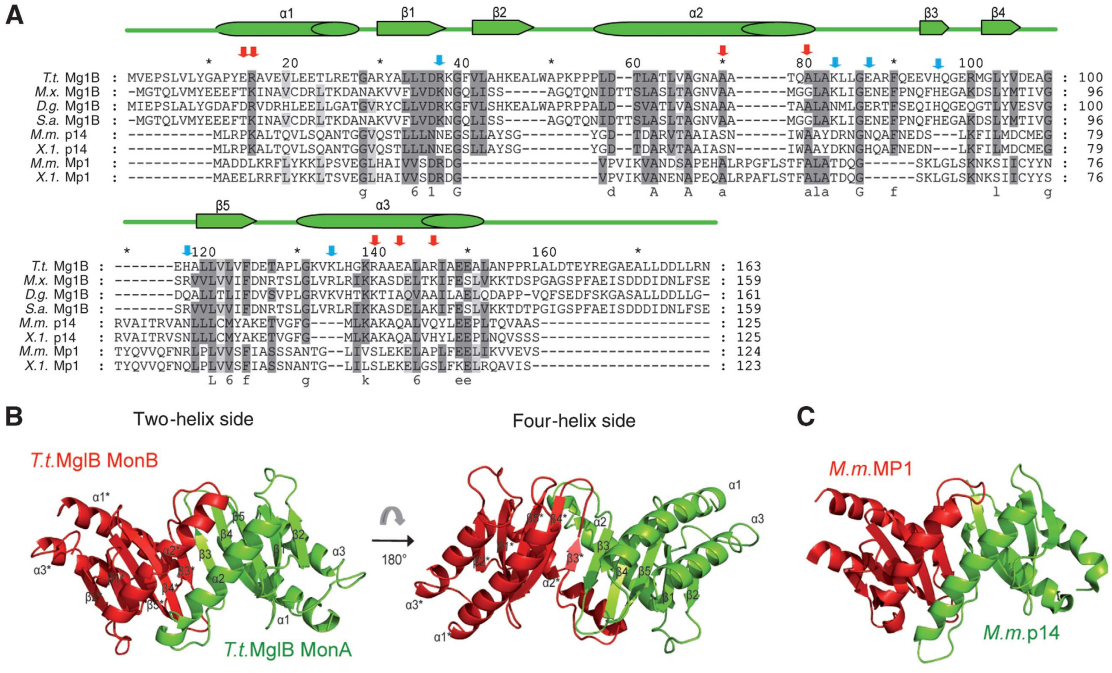

Figure 2 Structure of MglB. (**A**) Alignment of bacterial MglB from *M. xanthus* (*M.x.*), *T. thermophilus* (*T.t.*), *Deinococcus geothermalis* (*D.g.*) and *Stigmatella aurantiaca* (*S.a.*), with examples of the closest structural homologues, MP1 and p14, of *Mus musculus* (*M.m.*) and *Xenopus laevis* (*X.l.*). Conserved residues are highlighted in dark and light grey dependent on their degree of conservation. The secondary structure of MglB is indicated above the alignment. Red arrows show residues mutated for biochemical studies and crystallization purposes; blue arrows mark residues mutated without any effect on MglA binding, GAP activity or crystallization. (**B**) Homodimer of MgB with monomers (Mon) A (green) and B (red). The two-helix surface (left) and four-helix side (right) are related by 180°. (**C**) Heterodimer of Robl/LC7 domain proteins MP1 (red) and p14 (green) from *M. musculus* (1VEU). The two-helix side is shown.

space group C222(1) (Supplementary Table SI), four MglB monomers form a tetramer in the asymmetric unit (Supplementary Figure S3A). The space group and unit cell of these crystals is identical to those of MglB from *T. thermophilus* in the RCSB databank (1J3W). The MglB monomer has the Roadblock/LC7 fold of a five-stranded anti-parallel β-sheet sandwiched between the α2-helix on one side (Figure 2B, left) and terminal helices α1 and α3 on the other side (Figure 2B, right). MglB monomers dimerize via α2 and β3 thereby forming an extended anti-parallel β-sheet and giving rise to a two-helix side and a four-helix side of the dimer (Figure 2B). The two-helix sides of MglB dimers interact via α2 to form a tetramer via a four-helix bundle (Supplementary Figure S3A). In contrast, crystals belonging to space group P6(5)22 (Supplementary Table SI) contain only one MglB monomer in the asymmetric unit, which forms a β-sheet dimer via crystal contacts, but not a tetramer similar to the one in the C222(1) crystals (Supplementary Figure S3B). Instead, MglB oligomerizes by forming additional crystal contacts via α1, α3 which are also involved in crystal contacts to other MglB tetramers in the C222(1) crystals. Thus, the β-sheet dimer appears to be the smallest MglB building block.

Roadblock/LC7 proteins were reported as hetero- (MP1-p14) (Kurzbauer *et al*, 2004; Lunin *et al*, 2004) (Figure 2C) or homodimers (robl (Song *et al*, 2005), km23 (Ilangovan *et al*, 2005)) while the yeast p14/MP1 homologue Gse1p (Kogan *et al*, 2010) cannot form such a dimer due to its extra β3′-strand. Alignments with other Roadblock/LC7 proteins such as p14 and MP1 that were suggested by a DALI search to be the closest structural homologues shows only few conserved, mostly hydrophobic residues, which probably are important for the fold itself (Figure 2A). These residues are confined to contact interfaces observed in the MglB crystals, that is, the surface of MglB involved in β-sheet dimer formation and the surface of helix α2 engaged in tetramer formation (Supplementary Figure S4B). MglB proteins show no conserved arginine, asparagine or histidine residues that could potentially be involved in stimulation of GTP hydrolysis (Supplementary Figure S4A). Nevertheless, we mutated potentially catalytic residues including Glu14, Arg15, Arg37, Lys75, Glu79, His87, His102, Lys119, Arg124, Glu127 and Arg131. These mutations neither affected binding to MglA nor stimulation of GTP hydrolysis (unpublished observation), suggesting that MglB GAP activity is achieved via a mechanism different from those previously observed for Ras-like G proteins.

Structure of the MglA·GppNHp·MglB complex

Obtaining crystals for the complex of MglB bound to MglA in the active GppNHp state proved difficult. Crystals were readily obtained in 80% of screening conditions, but only contained MglB when analysed. We thus hypothesized that the surface of MglB is highly favourable to crystal packing as compared with the complex. Crystal contacts of MglB in the C222(1) and P6(5)22 crystals were mediated by helices α1 and α3. To eliminate these contacts, we introduced two substitutions in α3 where Arg124 and Glu127 were replaced with Ala. This mutant MglB readily crystallized in the presence of MglA·GppNHp, however, the crystals only contained MglB in space group I4(1) (Supplementary Figure S3C; Supplementary Table SII). Here, crystal contacts are mediated by helix α1. Consequently, an MglB mutant containing five substitutions in α1 and α3 was constructed by substituting Glu14, Arg15, Arg124, Glu127 and Arg131 with Ala (henceforth, $MglB^{A5}$).

Finally, a complex of MglA·GppNHp with $MglB^{A5}$ purified via size exclusion chromatography led to crystals of space group C222(1) (Supplementary Table SI), which contained both proteins, with one complex per asymmetric unit

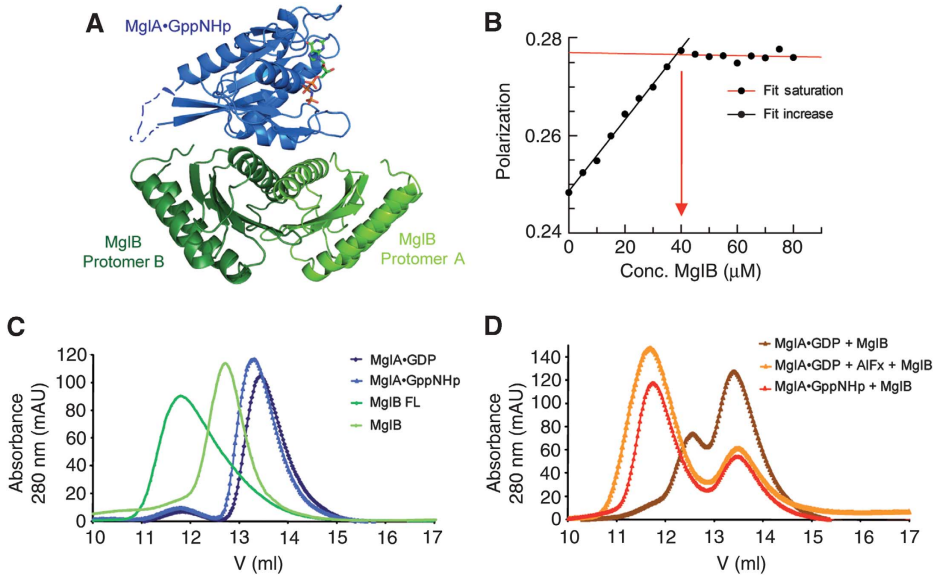

Figure 3 The MglA·GppNHp·MglB complex. (**A**) Structure of MglA·GppNHp (blue) bound to the $MglB^{A5}$ dimer (green/dark green). Flexible loops that were not visible in electron density are shown with dotted lines. (**B**) Active site titration. In all, 20 μM of MglA·mant-GppNHp were titrated with increasing amounts of MglB (K_d of 2 μM) at 37°C in Buffer M and the polarization increase was monitored. (**C**, **D**) Analytical size exclusion chromatography (Superdex 75 10/300 GL). (**C**) Elution profiles of MglB (light green), full-length MglB (dark green) and MglA bound to GDP (light blue) and GppNHp (dark blue). (**D**) MglA/MglB complex formation is monitored by mixing MglB with MglA·GppNHp (red) and MglA·GDP in presence (orange) or absence (brown) of AlFx as indicated.

(Figure 3A). Intriguingly, the complex is composed of one MglA molecule interacting with an MglB β-sheet dimer. MglA interaction with MglB is conveniently measured using *N*-methylanthraniloyl (mant)-labelled nucleotides. The 1:2 stoichiometry of the MglA·GppNHp·MglB^{A5} complex was confirmed by an active site titration in which MglA· mant-GppNHp (concentration above K_d) was titrated with increasing concentrations of MglB. Saturation of 20 μM MglA was observed with 40 μM MglB (monomer concentration) (Figure 3B). Formation of a 1:2 complex was further supported by analytical size exclusion chromatography (Figure 3C): MglB (M_w ca. 14 kDa) eluted before MglA, which eluted as a 22-kDa monomer independently of its nucleotide-bound state. This indicates the formation of multimers by MglB (and of MglB^{A5}; Supplementary Figure S5A). The elution volume of MglB is shifted to an apparent lower molecular mass with increasing salt concentrations, indicating increasing dissociation of the multimer (Supplementary Figure S2C). The symmetrical peak indicated a rapid monomer–dimer equilibrium. Upon complex formation with MglA·GppNHp, the elution volume shifted towards a higher molecular mass (Figure 3D). The elution volume best fits the molecular mass of a complex composed of one MglA and two MglB molecules. Other G-protein–cognate GAP complexes have a 1:1 stoichiometry and thus the MglA/MglB complex is the first G-protein–GAP complex reported to have a 1:2 stoichiometry.

Conformational changes and the GDP–GTP structural transition

The major feature of G-binding proteins as molecular switches is the conformational transition between the GDP- and GTP-bound conformations. Although the trigger for the structural change is canonical and originally defined to only include the two switch regions (Figure 1A), the degree of structural changes are different in different proteins and may also involve other parts of the protein (Vetter and Wittinghofer, 2001). In an overlay of the structures of MglA·GDP and MglA·GppNHp in the complex, large structural changes not previously observed in other G proteins are evident, although some elements of it have been observed in either Ran and Arf. In the absence of a structure of MglA bound to GppNHp alone, which we were unable to obtain, we cannot exclude that any of these structural changes have been induced or, more likely, stabilized by binding to GAP.

The superimposition shows that binding of inactive MglA·GDP to MglB would lead to steric clashes at the N-terminal β0-strand and switch I in MglA (Figure 4A). These steric clashes are relieved as a result of GppNHp binding and structural changes in both proteins. The β0-strand of MglA probably becomes flexible since no electron density could be detected. Its disappearance is accompanied by structural changes of one MglB protomer, which bends its α2 side more towards MglA (Figure 4E).

As in other G proteins, the GTP-induced structural changes involve switch I and II (Figure 4B and C). The extra β2*-strand of switch I persists in the GppNHp-bound state of MglA. This is in contrast to Ran where β2E becomes disordered upon GppNHp binding (Vetter *et al*, 1999). The most dramatic conformational change is the back-to-front movement of β2 in the β-sheet towards the nucleotide leading to a register shift by two amino acids (Figure 4D). The

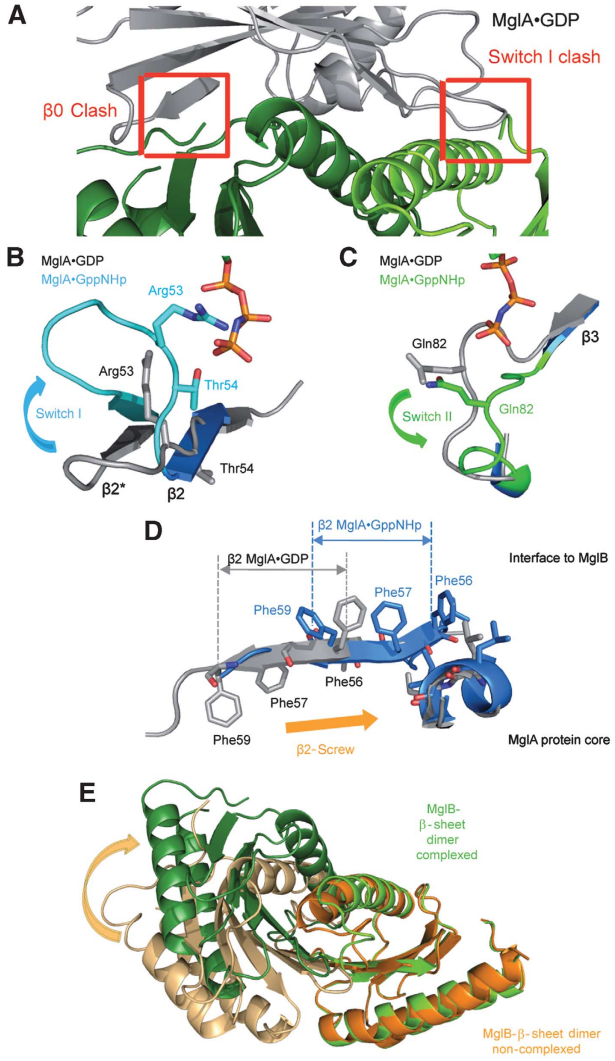

Figure 4 Conformational changes and the GDP–GTP structural transition. (**A**) Superimposition of MglA·GDP (grey) onto the MglA·GppNHp·MglB^{A5} structure shows how β0 and switch I would clash (red squares). (**B**) Structural change of switch I on the MglA·GDP (grey) to MglA·GppNHp (light blue) transition, highlighting Arg53 und Thr54. (**C**) Structural change of switch II on the MglA·GDP (grey) to MglA·GppNHp (light green) transition highlighting Gln82. (**D**) The β2-screw back-to-front (towards the nucleotide) movement of MglA on the GDP (grey) to GppNHp (blue) transition, reregistering Phe56, Phe57 and Phe59 besides other residues. (**E**) Structural changes of one MglB protomer in non-complexed MglB (light orange/orange), which bends its α2 side more towards MglA on complex formation (green/dark green).

back-to-front repositioning of β2 is accompanied by a 180° torsional movement/rotation. We refer to the movement of β2 as the β2-screw to distinguish it from a related register shift referred to as the interswitch toggle in Arf and Arl proteins that involves β2 as well as β3 and occurs front-to-back without a rotation upon GTP binding (Pasqualato *et al*, 2002). The β2-screw has several important consequences. First, it results in the exposure of Phe residues 57 and 59 on the MglA surface and allows these to make contact to MglB (Figure 4D). Second, it brings Thr54 into a position to establish the canonical Thr/γ-phosphate oxygen interaction of the G domain–GTP complex (Figure 4B). Third, it shifts the Arg53, which is absolutely conserved in MglA proteins, into a position where it contacts the γ-phosphate (Figure 4B;

Supplementary Movie S1). The effect of the β2-screw on the long (extra) loop connecting β2 and β3, which is expected to shorten upon repositioning of β2, is unclear since this loop could not be detected in the electron density map. The conformational changes in switch II are less dramatic but catalytically equally important as they involve the positioning of the conserved catalytic Gln82 of MglA towards the γ-phosphate and the nucleophilic water molecule (Figure 4C). The β0 conformational change is relatively distant and appears not to be caused by the γ-phosphate appearance but secondary to the GDP–GTP transition and the interaction with MglB.

The hydrophobic interface between MglA·GppNHp and MglB

The MglA·GppNHp·MglB^{A5} complex interface buries a 2044 Å^2 surface and is formed by β2*, β2, β3 and α2 from MglA and the two-helix side of the MglB dimer. There are a large number of interactions between the two proteins (schematically summarized in Figure 5A). The two monomers in the MglB dimer asymmetrically contact MglA and contribute to MglA binding with buried interfaces of 1310 and 765.29 Å^2, respectively. In the MglB dimer, α2 and α2* constitute the most important contact sites, with minor contributions from loops in both protomers. In MglA, the β2-screw repositions a stretch of hydrophobic amino acids on β2 (Leu55, Phe56, Phe57 and Phe59), some pointing inwards in MglA·GDP, towards the outside generating an extensive hydrophobic interface to MglB (Figures 4D and 5A). In contrast to other structures of Ras-like G proteins and their cognate GAPs, no residue from MglB reaches into the active site of MglA, confirming the absence of any conserved potential catalytic residue.

To further analyse the MglA/MglB interface, we introduced the double substitution A68/72R into the hydrophobic patch of α2 in MglB. MglA/MglB complex formation was measured as an increase in fluorescence polarization upon titration of MglB to MglA·mant-GppNHp (Figure 5B). The K_d of MglB$^{A68/72R}$ for MglA·GppNHp is about 34.6 μM, 10-fold lower than that of MglB (3.2 μM). Using the same assay, we verified that the MglB^{A5} mutant used for crystallization does not appreciably affect the affinity to MglA·GppNHp in line with the localization of the five substituted residues outside the MglA/MglB interface (Figure 5A and B). These results were also verified by analytical size exclusion chromatography in which MglB$^{A68/72R}$ was affected in complex formation with MglA while the MglB^{A5} mutant was not (Supplementary Figure S5A).

We also tested MglB-stimulated GTP hydrolysis on MglA using the [γ-^{32}P]GTP charcoal assay, which monitors release of inorganic $^{32}P_i$ (Figure 5C). Both MglB and MglB^{A5} stimulated the slow intrinsic GTP hydrolysis of MglA about 50-fold to about 0.005 μM s^{-1} while MglB$^{A68/72R}$ only stimulated GTP hydrolysis ∼10-fold even when the concentration of MglB$^{A68/72R}$ was increased to saturate complex formation (Figure 5C; Supplementary Figure S5B).

A new type of catalytic mechanism

Since Ras-like G proteins are considered incomplete enzymes, they require the presence of GAP to form a GDP–aluminium

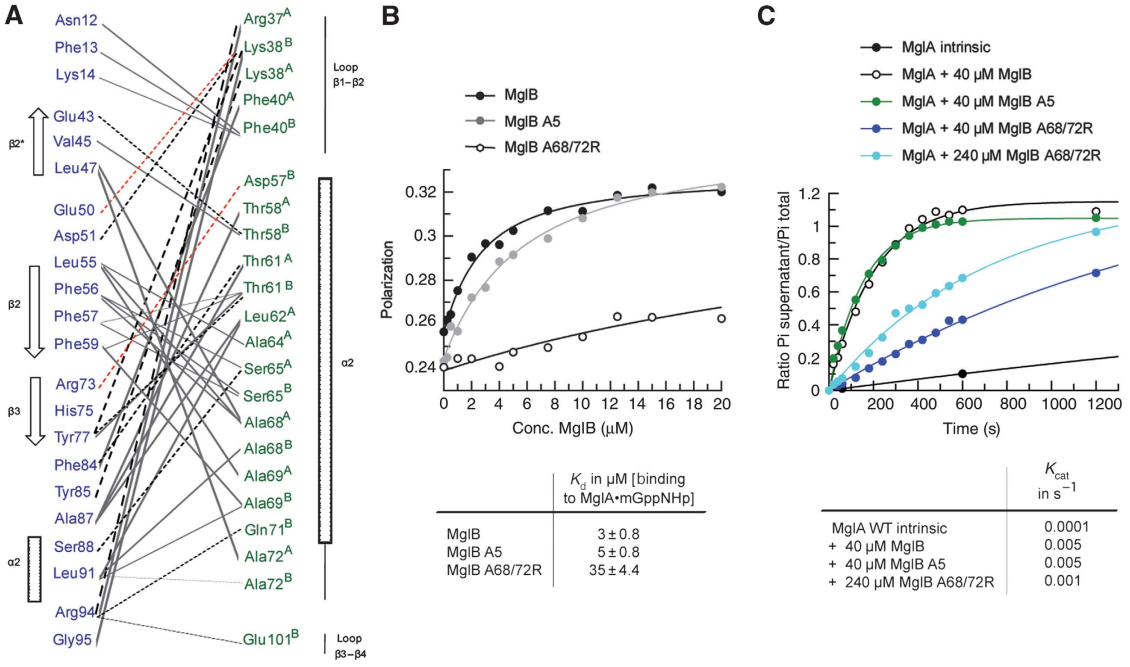

Figure 5 The hydrophobic interface between MglA·GppNHp and MglB. (**A**) Residues involved in interface between MglA (blue) and MglB Protomer A and B (green A, B) are schematically indicated. Hydrophobic and Van-der-Waals interactions (solid lines), salt bridges (red dotted lines) and H-bonds (black dotted lines) are shown. (**B**) Dissociation constants (K_d) determined by fluorescence polarization during titration of 1 μM MglA·mant-GppNHp with MglB, MglB$^{A68/72R}$ and MglB^{A5} at 37°C in Buffer M. One representative of three independently carried out experiments is shown. K_d's and error rates are the ones obtained by the fitting algorithm for the data shown. (**C**) Kinetics of GTP hydrolysis measured by Pi release from [γ-^{32}P]GTP by the Charcoal Assay at RT in Buffer M. Single turnover conditions were employed with 4 μM nucleotide-free MglA incubated with 1 μM GTP and 40 μM MglB, 40 μM MglB$^{A68/72R}$ or 240 μM MglB^{A5} thereby ensuring full complex formation. Data were plotted by showing the ratio of specific counts per minute of the supernatant over total counts per minute of sample at each time point. Hydrolysis rates (k_{cat}) were obtained by fitting data points to a first-order reaction using Grafit5 (Erithacus software).

fluoride (AlF_x) complex, which mimics the transition state of phosphoryl transfer (Mittal *et al*, 1996; Daumke *et al*, 2004; Gremer *et al*, 2008; Veltel *et al*, 2008a). This interaction is considered the lithmus test for whether a protein acts as a GAP or not (Gasper *et al*, 2009), and the structures of such complexes are the most appropriate way to elucidate the catalytic mechanism. We previously showed that MglB forms a complex with MglA·GDP in the presence of AlF_x (Leonardy *et al*, 2010).

Crystals of the MglA·GDP·AlF_4^-·$MglB^{A5}$ complex belong to space group C222(1) (Supplementary Table SI) and contained one complex per asymmetric unit. The structure is similar to that of the MglA·GppNHp·$MglB^{A5}$ complex (Figure 6A). MglA·GppNHp·$MglB^{A5}$ and MglA·GDP·AlF_4^-·$MglB^{A5}$ can be overlaid with an RMSD of 0.33 Å (441 Cα residues), with only a few minor changes in side chains. These subtle changes, however, are important to bring the catalytic components into more effective conformations.

While no Mg^{2+} was detected in the MglA·GDP conformation, it is present in the GppNHp conformation and forms a canonical bi-dentate complex with the β- and γ-phosphate oxygens. Its coordination is complemented by two water molecules and the side chains of Thr26 (P-loop) and Thr54 (switch I) (Figure 6B). Thr54 is brought into the correct position by the β2-screw during the GDP–GTP conformational change and/or MglB binding. Surprisingly, although Mg^{2+} coordination is as in most other Ras-like proteins, it does not seem to contribute to nucleotide affinity, since dissociation of mGppNHp is not affected by the presence of excess EDTA (10 mM, unpublished observation). The GDP–GTP conformational change also positions Gln82 in switch II closer towards the γ-phosphate allowing it to coordinate a water molecule for an in-line attack on the γ-phosphate. The most remarkable aspect of the active site is Arg53 in MglA, which also becomes positioned in the active site by the β2-screw in such a way that the bridging nitrogen of its guanidinium group contacts the γ-phosphate (Figure 6B). This intrinsic arginine is thus the potential substitute of the Arg-finger provided by most other GAPs cognate for Ras superfamily proteins.

In the transition state mimic, AlF_x occupies the γ-phosphate position and is modelled as AlF_4^- (Figure 6A and C). Aluminium is bound to the four fluoride ligands in a square planar coordination. Two oxygen atoms at the apical positions of an octahedron represent the leaving group and the attacking nucleophile of the hydrolysis reaction. Gln82 is moved slightly closer towards the nucleophilic water as compared with the GppNHp complex, thereby, reducing its distance to the γ-phosphate from 3.7 to 2.16 Å. Also, the guanidinium group of Arg53 contacts one fluoride via the bridging nitrogen Nε and another fluoride via the terminal nitrogen (Nω) (Figure 6C). As for other systems, the positive charge of the guanidinium group of Arg53 is believed to neutralize the developing charges on the γ-phosphate. This structure strongly suggests that Arg53 is indeed an intrinsic Arg-finger required to complete the catalytic site of MglA.

To verify the structural findings, we analysed the catalytic mechanism biochemically by substitution of MglA residues Gly21, Arg53 and Gln82. Gly21 is analogous to the Ras residue Gly12, which is often substituted in oncogenic Ras, and leads to loss of GAP-stimulated GTP hydrolysis (Leonardy *et al*, 2010). $MglA^{G21V}$, $MglA^{R53A}$ and $MglA^{Q82A}$ loaded with GppNHp bound to MglB with affinities similar to that of $MglA^{WT}$ as determined by fluorescence polarization (Figure 7A). Intrinsic and GAP-stimulated GTP hydrolysis as determined via the charcoal assay were completely abolished

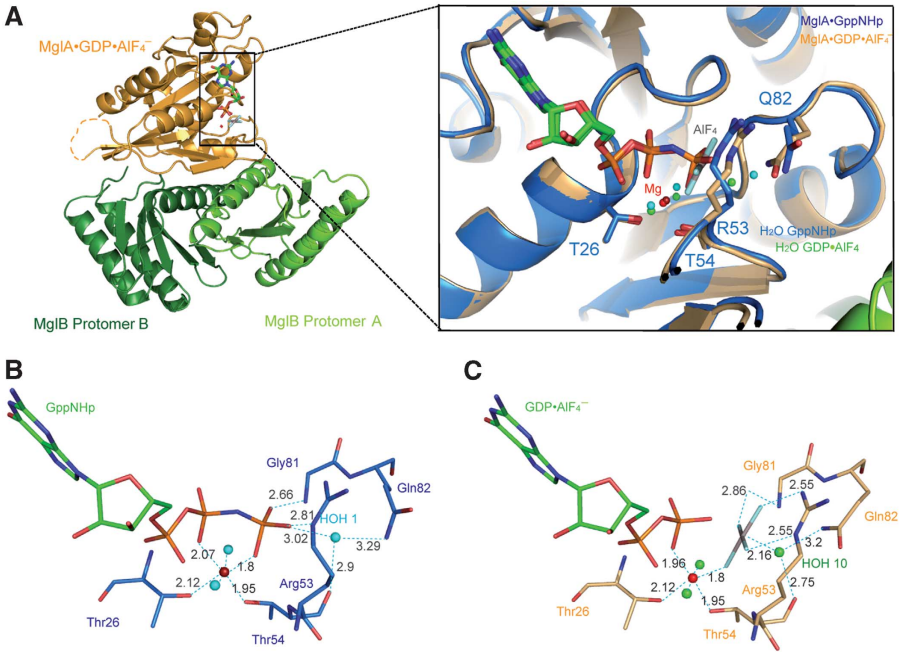

Figure 6 A new type of catalytic mechanism. (**A**) Structure of the MglA·GDP·AlF_4^-·$MglB^{A5}$ complex with MglA·GDP in yellow and $MglB^{A5}$ in green. Flexible loops not visible in the electron density are shown with dotted lines. Zoom into the active site of MglA·GDP·AlF_4^-·$MglB^{A5}$ (yellow) superimposed on MglA·GppNHp·$MglB^{A5}$ (blue). (**B**, **C**) Details of the active site of MglA·GppNHp·$MglB^{A5}$ (**B**) and comparison to MglA·GDP·AlF_4^-·$MglB^{A5}$ (**C**) Important residues, Thr26, Thr54, Gly81, Gln82 and Arg53, the catalytic water (blue dot) and distances in Angstroms (Å) are indicated.

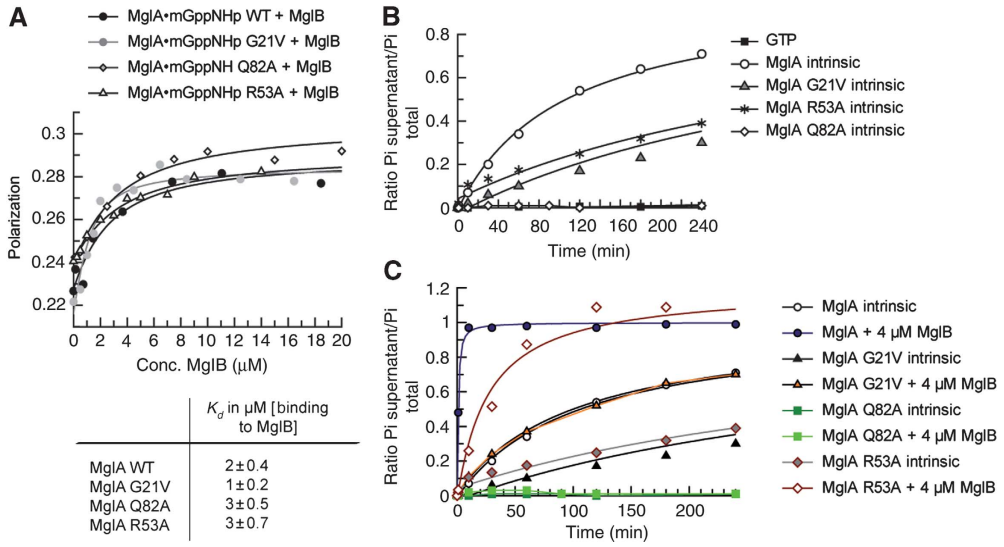

	K_d in μM [binding to MglB]
MglA WT	2±0.4
MglA G21V	1±0.2
MglA Q82A	3±0.5
MglA R53A	3±0.7

Figure 7 Mutational studies of the catalytic mechanism. (**A**) Dissociation constants (K_d) determined by fluorescence polarization by titrating 1 μM MglA^{WT}, MglA^{G21V}, MglA^{Q82A} and MglA^{R53A} bound to mant-GppNHp with MglB at 37°C in Buffer M. One representative of three independently carried out experiments is shown. K_d's and error rates, which are shown below, are the ones obtained by the fitting algorithm for the data shown. (**B**) Intrinsic hydrolysis of different mutants of MglA as described in Figure 5C. (**C**) GAP-stimulated GTP hydrolysis of MglA^{WT}, MglA^{G21V}, MglA^{Q82A} and MglA^{R53A} measured as described in Figure 5C. Single turnover conditions where 4 μM nucleotide-free MglA proteins were incubated with 1 μM GTP and equimolar amounts of GAP at RT in Buffer M.

in MglA^{Q82A} as previously reported for the MglA^{Q82L} mutant of the *M. xanthus* protein (Zhang *et al*, 2010) (Figure 7B), establishing it as the most important residue of GTP hydrolysis. Mutation of Arg53 in MglA reduces intrinsic as well as GAP-stimulated GTP hydrolysis to nearly the same extent as previously found for MglA^{G21V} (Leonardy *et al*, 2010). Thus, these data confirm that Arg53 is the intrinsic Arg-finger required to complete the catalytic site of MglA.

The MglA GTPase cycle regulates motility in M. xanthus

The function of MglA and MglB in *T. thermophilus* is not known and the expression of *T.t.mglBA* in a *M. xanthus* Δ*mglBA* mutant partially complements the motility defect (unpublished observation). Therefore, to rationalize the physiological relevance of the MglA GTPase cycle, we introduced the GTPase negative substitutions in *M. xanthus* MglA and MglB based on the conservation of relevant residues, and analysed the mutants for motility, reversals and protein localization. As reported (Leonardy *et al*, 2010; Zhang *et al*, 2010), *mglB*$^+$ cells containing YFP–MglA$^+$ occasionally reversed in a stochastic pattern with an average reversal period of 13.8 min (Table I). YFP–MglA$^+$ localized to the leading pole between reversals and relocated to the new leading pole during a reversal (Figure 8). In the absence of MglB, cells reversed two to three times more frequently in an oscillatory pattern and with YFP–MglA$^+$ localizing mostly in a bipolar pattern that did not change systematically during reversals (Table I; Supplementary Figure S6).

As previously reported for YFP–MglA^{G21V} and YFP–MglA^{Q82L} in *mglB*$^+$ cells (Leonardy *et al*, 2010; Zhang *et al*, 2010), YFP–MglA^{R53A} and YFP–MglA^{Q82A} complemented the motility defect in a Δ*mglA* mutant (Table I; Figure 8). *mglB*$^+$ and Δ*mglB* cells containing YFP–MglA^{G21V}, YFP–MglA^{R53A} or YFP–MglA^{Q82A} behaved similarly and reversed two to three times more frequently than cells containing YFP–MglA^{WT} in a highly regular, oscillatory pattern in which individual cells moved one cell length between reversals (Table I; Figure 8; Supplementary Figures S6 and S7). While the three GTPase negative proteins caused similar oscillatory motility behaviours, their localization was different. As previously reported (Leonardy *et al*, 2010), YFP–MglA^{G21V} forms a single cluster that oscillates between the cell poles (Figure 8). This cluster moves in the direction opposite to that of the cell, and arrival of the cluster at the lagging pole coincides with a reversal. YFP–MglA^{R53A} and YFP–MglA^{Q82A} localize in a bipolar pattern and also form an oscillating cluster moving between the poles as described for YFP–MglA^{G21V}.

MglB$^+$–YFP does not fully complement a Δ*mglB* mutation and cells reverse with an average period of 8.2 min. We therefore analysed the *M. xanthus* MglB$^{A64/G68R}$ mutant that corresponds to the *T.t.*MglB$^{A68/72R}$ mutant, which is unable to stimulate MglA GTPase activity, without YFP in Δ*mglB*$^+$ cells. We found that *M. xanthus* cells containing MglB$^{A64/G68R}$ reversed two to three times more frequently than wild-type (wt) cells in a regular oscillatory pattern (Table I). MglB$^+$–YFP localizes dynamically to the lagging pole in the presence of MglA, but in a bipolar pattern in the absence of MglA (Figure 8; Supplementary Figures S6 and S7). In contrast, MglB$^{A64/G68R}$–YFP localizes mostly in a bipolar pattern in the presence as well as in the absence of MglA. Thus, *mglA* and *mglB* mutations that result in reduced MglA GTPase activity phenocopy each other and cause a change in the occasional reversals in wt cells to a highly regular oscillatory pattern. Since the MglA mutant proteins still interact efficiently with MglB as shown *in vitro* (Figure 7), the interaction between MglA and MglB that regulates reversal frequency and localization apparently depend on MglB GAP activity. Cells containing MglB^{A5}, which have wt GAP activity, have a wt reversal frequency but MglB^{A5}–YFP localization is slightly more diffuse (Table I; Figure 8). Since the A5 mutant cannot interact via the α1, α3 region, this suggests that polymerization of MglB dimers via α1, α3 is not essential for MglB function.

Table I Characterization of MglA and MglB mutants *in vivo*

Strain	Relevant genotype	Reversal period (min)	Cluster localization between reversals				Cluster localization during reversals
			Unipolar	Bipolar	Bipolar and oscillating[a]	Oscillating[a]	
DK1622	*mglB*$^{+}$ *A*$^{+}$	15.7 ± 4.6					
DK6204	Δ*mglBA*	Non-motile					
SA4420	Δ*mglA*	Non-motile					
SA3397	Δ*mglB*	6.7 ± 0.8					
SA3955	*mglB*^{A5}	17.4 ± 3.1					
SA3954	*mglB*$^{A64/G68R}$	6.4 ± 0.5					
SA4440	Δ*mglA/yfp–mglA*$^{+}$	13.8 ± 3.2	84[b]	16[b]	—	—	Unipolar cluster dynamic
SA4451	Δ*mglA/yfp–mglA*^{G21V}	4.6 ± 0.3	11	—	—	89	Oscillating cluster 'hits' lagging pole
SA4445	Δ*mglA/yfp–mglA*^{R53A}	5.9 ± 0.8	—	30	70	—	Oscillating cluster 'hits' lagging pole
SA3829	Δ*mglA/yfp–mglA*^{Q82A}	6.9 ± 0.1	8	—	92	—	Oscillating cluster 'hits' lagging pole
SA3385	Δ*mglBA/yfp–mglA*$^{+}$	7.7 ± 0.9	28[b]	72[b]	—	—	Stationary
SA3823	Δ*mglBA/yfp–mglA*^{G21V}	5.9 ± 0.3	7	—	0	93	Oscillating cluster 'hits' lagging pole
SA4449	Δ*mglBA/yfp–mglA*^{R53A}	6.5 ± 0.3	3	—	97	—	Oscillating cluster 'hits' lagging pole
SA3831	Δ*mglBA/yfp–mglA*^{Q82A}	7.1 ± 0.4	7	—	93	—	Oscillating cluster 'hits' lagging pole
SA3388	Δ*mglB/mglB*$^{+}$*–yfp*	8.2 ± 1.0	80	20			Unipolar cluster dynamic
SA3951	Δ*mglB/mglB*^{A5}*–yfp*	7.8 ± 0.6	67[c]	33[c]			Unipolar cluster dynamic
SA3950	Δ*mglB/mglB*$^{A64/G68R}$*–yfp*	6.9 ± 0.3	32	68			Stationary
SA3383	Δ*mglBA/mglB*$^{+}$*–yfp*	Non-motile	40	60			NA
SA3953	Δ*mglBA/mglB*^{A5}*–yfp*	Non-motile	37[c]	63[c]			NA
SA3952	Δ*mglBA/mglB*$^{A64/G68R}$*–yfp*	Non-motile	48	52			NA

[a]The arrow at the central cluster indicates that the cluster relocates towards lagging cell pole between reversals.
[b]Cells expressing YFP–MglA^{+} have a strong diffuse signal.
[c]Cells expressing MglB^{A5}–YFP have a diffuse signal.

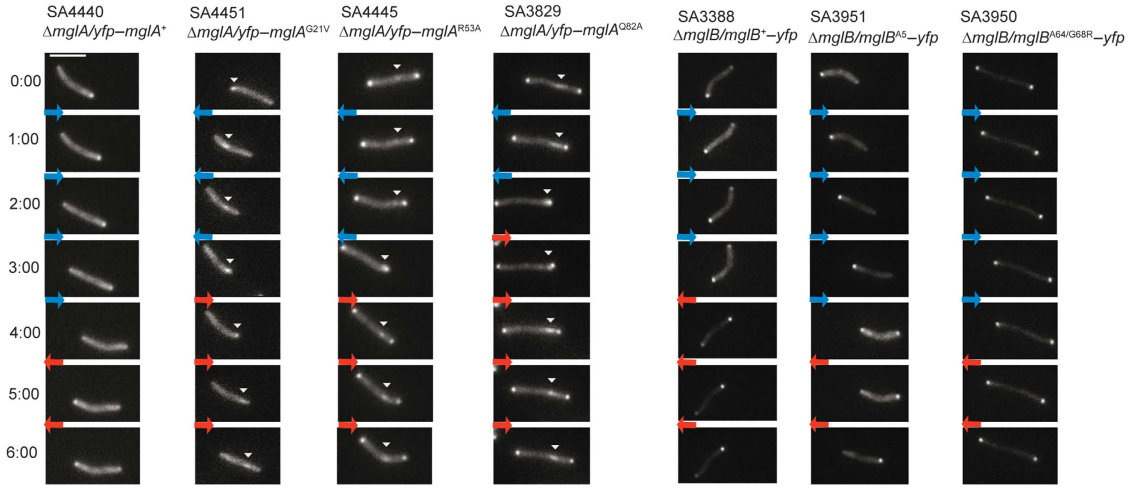

Figure 8 MglA GTPase activity and MglB GAP activity are essential for correct localization. Strains of the indicated genotypes were transferred from exponentially growing cultures to a thin agar-pad on a microscope slide, and imaged by time-lapse fluorescence microscopy. Red and blue arrows indicate opposite directions of movement. White arrowheads indicate the oscillating cluster generated by the three mutant MglA proteins.

Discussion

By sequence and structural homology, MglA proteins seem to constitute an extra branch of the Ras superfamily. Structurally, four unique characteristics separate MglA from other known Ras-like proteins: First, it has an extra β-strand (β2*) on the edge of the β-sheet corresponding to switch I, which unlike in Ran does not disappear after the GDP–GTP conformational transition. Second, β2 in the central β-sheet undergoes an exceptional GDP–GTP-dependent structural transition in which the β2-screw movement brings γ-phosphate binding residues in switch I and II, Thr54 and Gly81, into their canonical position (Vetter and Wittinghofer, 2001). However, whether the β2-screw is solely the consequence of the GDP–GTP-dependent conformational change or requires the interaction with GAP remains unresolved, as we have not

been able to crystallize and solve the structure of the MglA·GppNHp complex. Nevertheless, it is tempting to speculate that, as in Arf and Arl proteins, where the presence of the γ-phosphate induces the movement of switch I, II and the interswitch toggle, the β2-screw is the result of the structural transition of MglA between its GDP- and GTP-bound forms. This is supported by our finding that the β2-screw movement is required to position crucial hydrophobic residues such as Leu55, Phe56, Phe57 and Phe59 involved in the MglA–MglB interface. This scenario does not exclude that the presence of a GAP or a possible hitherto unknown effector might stabilize an otherwise highly dynamic GTP-bound conformation, in particular since the affinity of MglA to GTP/GppNHp is estimated to be 100-fold weaker than to GDP.

Third, MglA is also unique among Ras proteins in that it contains the two catalytic residues, Arg53 and Gln82, which are brought into position by the GDP–GTP conformational transition. In particular, Arg53 is brought into γ-phosphate binding distance by the β2-screw. Fourth, MglB does not directly participate in catalysis but rather stabilizes and/or properly orients the catalytic machinery. This is reminiscent of Gα proteins, which also contain an intrinsic Gln in switch II and Arg in switch I (Sprang, 1997; Sprang *et al*, 2007). Here, stabilization and GTPase stimulation is mediated by RGS proteins and sometimes additionally by binding to effector proteins. Comparison of the MglA–MglB and $G_{i\alpha1}$–RGS4 complexes (Tesmer *et al*, 1997) shows some similarities and minor differences (Supplementary Figure S8). In both cases, the catalytic glutamine residues superimpose very well, while the catalytic arginines reach into the active sites from different directions, as observed for the comparison between the Ras–RasGAP system and the G_i–RGS complex (Scheffzek *et al*, 1997a). RGS4 is close to the active site of $G_{i\alpha1}$ and points an Asn towards the active site of $G_{i\alpha1}$ (Tesmer *et al*, 1997), while no residue of MglB comes even close to the active site of MglA. Mutation of several interface residues of RGS4 affects catalysis indirectly by lowering the affinity between the proteins arguing that in both cases the stabilization of the intrinsic machinery by complex formation is the prevalent mechanism (Srinivasa *et al*, 1998). Binding of MglA to MglB and binding of G proteins to RGS occur with highest affinity to the GDP·AlF_4^- state. Both RGS4 and MglB binding leads to an $\sim 10^2$-fold stimulation of the GTPase activity of $G_{i\alpha1}$ and MglA, respectively. As $G_{i\alpha1}$ and MglA possess a full catalytic machinery already, this might explain, why only a 10^2-fold increase in MglA GTPase activity by MglB can be observed, in contrast to eukaryotic Ras-like G proteins, for which a 10^5-fold stimulation of GTPase activity by its cognate GAPs is commonly observed (Spoerner *et al*, 2001; Bos *et al*, 2007).

MglB as the member of Roadblock/LC7 fold is the founding member of a new family of GAPs (Koonin and Aravind, 2000; Kurzbauer *et al*, 2004; Lunin *et al*, 2004; Song *et al*, 2005). In the MglA/MglB complex, MglB interacts with MglA in a 2:1 stoichiometry that has not been observed before. While RapGAP1 is a constitutive dimer, it forms a 2:2 complex with Rap1 and dimer formation is not necessary for RapGAP activity (Daumke *et al*, 2004; Scrima *et al*, 2008). Likewise, dimeric RopGAP2 is a dimer in solution but it also forms a 2:2 complex with Rops (Schaefer *et al*, 2011). Various crystal structures of MglB suggested that in addition to forming a dimer via the interprotein β-sheet interaction, MglB also has a tendency to form higher oligomers in solution, which is particularly apparent from the size exclusion chromatography experiment using full-length protein (Figure 3C; Supplementary Figure S2C). *In vivo* experiments with wt MglB and the A5 mutant indicate that motility, reversal period and localization are not appreciably affected by substitutions that interfere with polymerization of MglB dimers via the α1, α3 region, suggesting that polymers observed in the crystals are not biologically relevant.

Not much is known about the mechanistic function of other members of the LC7/Roadblock family. Roadblock/LC7, LC8 and Tctex1/rp3/Tctex2 are distinct classes of the dynein light chain family and may be involved in the ATP function of dynein during minus end-directed transport along microtubules (Kardon and Vale, 2009). The complex between MP1/p14, which was originally implicated in the regulation of MAP kinase signalling, has recently been shown to form a trimeric complex with p18 (Sancak *et al*, 2010). This trimeric complex called Ragulator seems to regulate the function of Rag proteins of the Ras superfamily, similar to what is presumed for the yeast Gse1p/Gse2p complex acting on the Rag homologues Gtr1p–Gtr2p (Dubouloz *et al*, 2005; Gao and Kaiser, 2006; Zurita-Martinez *et al*, 2007; Kogan *et al*, 2010).

Cells of *M. xanthus* organize in two different patterns, in the presence of nutrient cells organize to form spreading colonies and in the absence of nutrients cells aggregate to form multicellular fruiting bodies. Formation of both patterns depends on regulation of the reversal frequency (Blackhart and Zusman, 1985). Reversals are induced by the Frz chemosensory system and in a constant environment reversals are random events that allow cellular net-movement because reversal periods vary widely. In the absence of nutrients, reversals are inhibited by the intercellular C-signal (Jelsbak and Søgaard-Andersen, 2002). It was previously shown that in the absence of Frz activity, the MglA/MglB system establishes a stable leading/lagging pole polarity axis resulting in uni-directional movements and this axis is inverted in response to Frz activity (Leonardy *et al*, 2010; Zhang *et al*, 2010). Guided by the crystal structures of MglA and MglB, we introduced substitutions in MglA from *M. xanthus* that inactivated the GTPase activity of MglA as well as substitutions in MglB from *M. xanthus* that strongly reduce binding of MglB to MglA. Our data show that if MglA GTPase activity is compromised by substitutions in either MglA or MglB, cells are still motile; however, cells change their reversal pattern to a highly regular oscillatory pattern and are unable to display net-movement because they only move a single cell length before reversing. These observations demonstrate that in the absence of MglA GTPase activity, the leading/lagging polarity axis is not stably maintained over extended periods of time but changes regularly. Therefore, the design of the wt MglA/MglB polarity system accommodates both a stable polarity axis (between reversals) that depends on regulation of MglA GTPase activity by MglB, and a dynamic polarity axis that depends on Frz activity.

The wt MglA and MglB proteins localize in clusters at the leading and lagging cell pole, respectively, and relocate to the opposite pole during a reversal. It is not known how MglA and MglB bind to the cell poles. The previous observations that both MglA and MglB bind in a bipolar pattern in the absence of the other or in case of an impaired MglA GTPase activity in the case of $MglA^{R53A}$, $MglA^{Q82A}$ and $MglB^{A64/R68R}$ have important implications: First, these observations sug-

gest that landmark proteins required for polar binding of MglA and MglB are present at both poles at the same time. Second, the asymmetric polar localization of the wt proteins is not the result of competition for the same binding sites but rather the result of MglA GTPase activity and MglB GAP activity. The two MglA GTPase mutants YFP–MglA^{R53A} and YFP–MglA^{Q82A} localize in a similar pattern with the formation of bipolar clusters as well as a cluster that oscillates regularly between the cell poles while the YFP–MglA^{G21V} GTPase mutant forms a regularly oscillating cluster. The different localization patterns of YFP–MglA^{G21V}, YFP–MglA^{R53A} and YFP–MglA^{Q82A} indicate that the interaction to landmark proteins at the cell poles is differently affected by the substitutions. Formation of the oscillating cluster involves MglA·GTP and most likely depends on the interaction with effector proteins. We speculate that the different localization patterns of MglA^{G21V}, MglA^{R53A} and MglA^{Q82A} might be caused by differential effector interactions due to surface charge changes in the switch I and II regions through these mutations. We do not know how the oscillating cluster results in reversals. However, we speculate that the cluster brings cargo to the lagging cell pole and that this causes the reversal.

Materials and methods

Construction of plasmids and strains, cell growth, antibody generation, immunoblot analysis and biochemical methods

These procedures are described in the Supplementary data. A list of strains is given in Supplementary Table SV.

Plasmids and protein purification

(Leonardy *et al*, 2010) Homologues of the *M. xanthus* MglA and MglB proteins were amplified by PCR out of a DNA library from *T. thermophilus* HB8. In this work, shortened MglB comprising amino acids 6–139 (intrinsic G65S mutation) was used. The genes were cloned into pGexET (derivative of pGex4T-1) containing an N-terminal Glutathione-S-transferase fusion followed by a thrombin cleavage site. Respective MglA^{G21V}, MglA^{Q82A}, MglA^{R53A} and MglB$^{A68/72R}$, MglB$^{R124/E127A}$ and MglB^{A5} (A5 = E14/R15/R124/E127/R131A) mutants were generated by mutagenesis PCR. All proteins were expressed in BL21 DE3 codon plus RIL cells at 18°C following induction with 100 μM IPTG overnight. Purification was done using GSH-sepharose columns (Amersham/GE Healthcare), which were washed with Wash-Buffer (25 mM Tris–HCl pH 7.5, 500 mM NaCl, 5 mM $MgCl_2$, 5 mM DTE and 10% glycerol). The GST-fusion proteins were eluted with Elution-Buffer (Wash-Buffer + 20 mM reduced glutathione). Following cleavage with thrombin overnight and removal of residual GST, size exclusion chromatography was performed using a Superdex 75 26/60 (Amersham/GE Healthcare). The proteins were stored in Buffer M containing 50 mM Tris pH 7.5, 50 mM NaCl, 5 mM $MgCl_2$, 1 mM DTE and 5% glycerol.

Crystallization

Native and Seleno-methionine (Se-Met)-labelled MglA were purified according to the procedure mentioned above, except that the amount of DTE was increased to 10 mM in all buffers for Se-Met MglA. Proteins had GDP bound and were concentrated to 15 mg ml^{-1}. The sitting drop/vapour diffusion method was used and an initial condition was found in EasyXtal CLASSIC I Suite from Qiagen. The condition
was optimized to a final solution of 65% MPD and 0.1 M Tris pH 8.5. Se-Met crystals of space group P1 and P2(1) (Supplementary Table SII) were not readily reproducible and microseeding had to be employed (Scheffzek *et al*, 1997b; Bergfors, 2003).

Crystallization of MglB. MglB samples (derived from MglA/MglB complex purification) were concentrated to about 15 mg ml^{-1} in each case. The sitting drop/vapour diffusion method was used and crystals of space group C222(1), P6(5)22 (Supplementary Table SI) and I4(1) (Supplementary Table SII) appeared in initial conditions of the EasyXtal JCSG CORE I, CORE II or CORE IV Suites from Qiagen, respectively. For C222(1) crystals, the condition was optimized to a final solution of 0.1 M $MgCl_2$, 2.5 M NaCl and 0.1 M Tris–HCl pH 7.0, for P6(5)22 to 0.28 M $CaCl_2$, 7% Isopropanol, 30% Glycerol and 0.07 M Natrium-Acetate pH 4.6 and for I4(1) to 0.1 M CHES and 30% PEG400 pH 9.5.

Crystallization of MglA/MglB was achieved by incubation of nucleotide-free MglA with a two-fold molar excess of GppNHp and equimolar amounts of MglB^{A5} for 15 min at RT, which was then run on a Superdex 75 10/300 in Buffer M. The fractions containing the complex were pooled and concentrated to 10.6 mg ml^{-1}. In order to crystallize the MglA/MglB complex in the transition state, nucleotide-free MglA was mixed with a two-fold molar excess of GDP and an equimolar amount of MglB^{A5} in the presence of 2 mM AlFx. The sample was concentrated to 8.5 mg ml^{-1} and directly used for crystallization. The sitting drop/vapour diffusion method was used and an initial condition was found in EasyXtal JCSG CORE III Suite from Qiagen for both complexes. For MglA·GppNHp·MglB^{A5}, the condition was optimized to a final solution of 1.25 M LiCl, 0.1 M Hepes and 15% PEG6000 pH 7.0 and for MglA·GDP·AlF_4^-·MglB^{A5} to a final solution of 0.2 M $MgCl_2$, 0.1 M Tris and 15% PEG8000 pH 8.5.

In all cases, crystals usually appeared after 1–3 days and were flash frozen after 3 days in a cryosolution containing the same constituents as the crystallizing condition supplemented with glycerol; except for MglA crystals for which MPD was already cryoprotectant. Data collection were done at the PXII-X10SA beamline of the Swiss Light Source (SLS), Villigen. Only data for the MglA·GppNHp·MglB^{A5} crystal were collected at the ID23-2 beamline of the European Synchrotron Radiation Facility (ESRF), Grenoble. Type and wavelength of the beamline used are indicated in Supplementary Tables SI and SII.

Data were indexed and processed with XDS (Kabsch, 1993). Molecular Replacement was done with MOLREP and PHASER from the CCP4 package. For the Se-Met data set of MglA in space group P2(1) heavy atom sites for SAD phasing were identified with SOLVE (Terwilliger, 2002) and an initial model was calculated with RESOLVE (Terwilliger, 2002). Density was improved using four-fold averaging with DM. The model was completed with help of buccaneer and further refined with REFMAC5 (Murshudov *et al*, 1997) and COOT (Emsley and Cowtan, 2004). The raw model from SAD phasing was used to solve the higher resolution native P1 structure (Supplementary Table SI) and the P1 Se-Met data set (Supplementary Table SII) using MOLREP and PHASER. In case of the complexes, one monomer of our own MglA structure and one monomer of the MglB (1J3W) structure were used with MOLREP; the nucleotide was not included in the search model in case of MglA and the complexes. The different structures were refined using REFMAC5 (Murshudov *et al*, 1997) to following resolutions [Ramachandran statistics in brackets]: MglA native to 1.9 Å [98.4% favoured, 1.6% allowed, 0% outlier]; MglA Se-Met P1 to 1.9 Å [98.0% favoured, 2% allowed, 0% outlier]; MglA Se-Met P2(1) to 2.4 Å [97.2% favoured, 2.8% allowed, 0% outlier]; Crystals for MglB of C222(1) to 2.0 Å [98.3% favoured, 1.7% allowed, 0% outlier]; of P6(5)22 to 1.67 Å [98.5% favoured, 1.5% allowed, 0% outlier]; MglA·GppNHp·MglB^{A5} complex to 2.7 Å [97.2% favoured, 2.8% allowed, 0% outlier] and MglA·GDP·AlF_4^-·MglB^{A5} complex to 2.2 Å [97.7% favoured, 2.3% allowed, 0% outlier]. For data and refinement statistics, see Supplementary Tables SI and SII. All the figures were produced using PYMOL (DeLano Scientific LLC). Atomic coordinates and structural factors have been deposited within the Research Collaboratory for Structural Bioinformatics (RCSB) Protein Data Bank (PDB) under the following accession codes: 3T12 (MglA·GDP·AlF_4-·MglB^{A5}), 3T1Q (MglA·GppNHp·MglB^{A5}), 3T1O (MglA·GDP), 3T1R (MglB Tetramer), 3T1S (MglB Monomer), 3T1X (MglB$^{R124/E127A}$), 3T1T (MglA·GDP tetrameric arrangement P1) and 3T1V (MglA·GDP tetrameric arrangement P2(1).

Microscopy and determination of reversal periods

For microscopy, *M. xanthus* cells were grown and treated for time-lapse microscopy as described (Leonardy *et al*, 2007; Bulyha *et al*, 2009). Cells were placed on a thin 0.7% agar-pad buffered with A50

starvation buffer (10 mM MOPS pH 7.2, 10 mM $CaCl_2$, 10 mM $MgCl_2$, 50 mM NaCl) on a glass slide and immediately covered with a cover slip, and then imaged at 30 s intervals for 10–15 min. Images were recorded and processed with Leica FW4000 V1.2.1 or Image Pro 6.2 (MediaCybernetics) software. Processed images were visualized in Metamorph 7.0r2 software (Molecular Devices). To calculate reversal periods, the total number of moving cells was multiplied by the elapsed time and divided by the number of reversals. At least 100 cells were analysed per experiment.

Supplementary data

Supplementary data are available at *The EMBO Journal* Online (http://www.embojournal.org).

Acknowledgements

We thank Toni Meinhardt, Andrea Rocker, Eckhard Hofmann, Marco Bürger, Ilme Schlichting, Thomas Barends, Christian Grütter, Björn Over, Brad Lunde and the SLS beamline staff for data collection of the many crystals at the Swiss Light Source, beamline PXII-X10SA, Paul Scherrer Institute, Villigen, Switzerland and Marco Bürger, Eckhard Hofmann and the ESRF beamline staff for data collection at the ESRF, beamline ID23-2, in Grenoble, France. We also thank Shehab Ismail for excellent scientific discussions. We further thank Tim Schöner for help with the construction of plasmids encoding YFP–$MglA^{Q82A}$. This work was supported by The Max-Planck Society, the graduate programme 'Intra- and intercellular transport and communication' funded by the German Research Foundation, the SFB Nr 642 (to AW) and the LOEWE Research Center for Synthetic Microbiology.

Author contributions: MM contributed to protein preparation, biochemical/biophysical measurements, crystallization, X-ray data analysis and manuscript preparation; CK contributed to cloning and protein preparation; IRV performed crucial help with X-ray data analysis; DK contributed to cell assays and analysis of MglB mutants; EH and SL contributed to cell assays and analysis of MglA mutants; LSA and AW contributed to project design, supervision and manuscript preparation.

Conflict of interest

The authors declare that they have no conflict of interest.

References

Ahnn J, March PE, Takiff HE, Inouye M (1986) A GTP-binding protein of Escherichia coli has homology to yeast RAS proteins. *PNAS* **83:** 8849–8853

Alto NM (2008) Mimicking small G-proteins: an emerging theme from the bacterial virulence arsenal. *Cell Microbiol* **10:** 566–575

Bergfors T (2003) Seeds to crystals. *J Struct Biol* **142:** 66–76

Blackhart BD, Zusman DR (1985) 'Frizzy' genes of Myxococcus xanthus are involved in control of frequency of reversal of gliding motility. *PNAS* **82:** 8767–8770

Bos JL, Rehmann H, Wittinghofer A (2007) GEFs and GAPs: critical elements in the control of small G proteins. *Cell* **129:** 865–877

Brown ED (2005) Conserved P-loop GTPases of unknown function in bacteria: an emerging and vital ensemble in bacterial physiology 1. *Cell* **746:** 738–746

Bulyha I, Schmidt C, Lenz P, Jakovljevic V, Höne A, Maier B, Hoppert M, Søgaard-Andersen L (2009) Regulation of the type IV pili molecular machine by dynamic localization of two motor proteins. *Mol Microbiol* **74:** 691–706

Clausen M, Jakovljevic V, Søgaard-Andersen L, Maier B (2009) High-force generation is a conserved property of type IV pilus systems. *J Bacteriol* **191:** 4633–4638

Cox AD, Der CJ (2010) Ras history. *Small GTPases* **1:** 2–27

Daumke O, Weyand M, Chakrabarti PP, Vetter IR, Wittinghofer A (2004) The GTPase-activating protein Rap1GAP uses a catalytic asparagine. *Nature* **429:** 197–201

Dubouloz F, Deloche O, Wanke V, Cameroni E, De Virgilio C (2005) The TOR and EGO protein complexes orchestrate microautophagy in yeast. *Mol Cell* **19:** 15–26

Emsley P, Cowtan K (2004) Coot: model-building tools for molecular graphics. *Acta Crystallogr D Biol Crystallogr* **60:** 2126–2132

Gao M, Kaiser CA (2006) A conserved GTPase-containing complex is required for intracellular sorting of the general amino-acid permease in yeast. *Nat Cell Biol* **8:** 657–667

Gasper R, Meyer S, Gotthardt K, Sirajuddin M, Wittinghofer A (2009) It takes two to tango: regulation of G proteins by dimerization. *Nat Rev Mol Cell Biol* **10:** 423–429

Gremer L, Gilsbach B, Ahmadian MR, Wittinghofer A (2008) Fluoride complexes of oncogenic Ras mutants to study the Ras-RasGap interaction. *Biol Chem* **389:** 1163–1171

Herrmann C (2003) Ras-effector interactions: after one decade. *Curr Opin Struct Biol* **13:** 122–129

Hillig RC, Hanzal-Bayer M, Linari M, Becker J, Wittinghofer A, Renault L (2000) Structural and biochemical properties show ARL3-GDP as a distinct GTP binding protein. *Structure* **8:** 1239–1245

Hwang J, Inouye M (2010) A bacterial GAP-like protein, YihI, regulating the GTPase of Der, an essential GTP-binding protein in Escherichia coli. *J Mol Biol* **399:** 759–772

Ilangovan U, Ding W, Zhong Y, Wilson CL, Groppe JC, Trbovich JT, Zúñiga J, Demeler B, Tang Q, Gao G, Mulder KM, Hinck AP (2005) Structure and dynamics of the homodimeric dynein light chain km23. *J Mol Biol* **352:** 338–354

Inoki K, Li Y, Xu T, Guan K-L (2003) Rheb GTPase is a direct target of TSC2 GAP activity and regulates mTOR signaling. *Genes Dev* **17:** 1829–1834

Jelsbak L, Søgaard-Andersen L (2002) Pattern formation by a cell surface-associated morphogen in Myxococcus xanthus. *PNAS* **99:** 2032–2037

Kabsch W (1993) Automatic processing of rotation diffraction data from crystals of initially unknown symmetry and cell constants. *J Appl Chrystallogr* **26:** 795–800

Kardon JR, Vale RD (2009) Regulators of the cytoplasmic dynein motor. *Nat Rev Mol Cell Biol* **10:** 854–865

Kogan K, Spear ED, Kaiser CA, Fass D (2010) Structural conservation of components in the amino acid sensing branch of the TOR pathway in yeast and mammals. *J Mol Biol* **402:** 388–398

Koonin EV, Aravind L (2000) Dynein light chains of the Roadblock/LC7 group belong to an ancient protein superfamily implicated in NTPase regulation. *Curr Biol* **10:** R774–R776

Kurzbauer R, Teis D, Araujo MEGD, Maurer-stroh S, Eisenhaber F, Bourenkov GP, Bartunik HD, Hekman M, Rapp UR, Huber LA, Clausen T (2004) Crystal structure of the p14-MP1 scaffolding complex: how a twin couple attaches mitogen-activated protein kinase signaling to late endosomes. *PNAS* **101:** 10984–10989

Leonardy S, Bulyha I, Søgaard-Andersen L (2008) Reversing cells and oscillating motility proteins. *Mol Biosyst* **4:** 1009–1014

Leonardy S, Freymark G, Hebener S, Ellehauge E, Søgaard-Andersen L (2007) Coupling of protein localization and cell movements by a dynamically localized response regulator in Myxococcus xanthus. *EMBO J* **26:** 4433–4444

Leonardy S, Miertzschke M, Bulyha I, Sperling E, Wittinghofer A, Søgaard-Andersen L (2010) Regulation of dynamic polarity switching in bacteria by a Ras-like G-protein and its cognate GAP. *EMBO J* **29:** 2276–2289

Lunin VV, Munger C, Wagner J, Ye Z, Cygler M, Sacher M (2004) The structure of the MAPK scaffold, MP1, bound to its partner, p14. A complex with a critical role in endosomal map kinase signaling. *J Biol Chem* **279:** 23422–23430

Mehr IJ, Long CD, Serkin CD, Seifert HS (2000) A homologue of the recombination-dependent growth gene, rdgC, is involved in gonococcal pilin antigenic variation. *Genetics* **154:** 523–532

Merz AJ, So M, Sheetz MP (2000) Pilus retraction powers bacterial twitching motility. *Nature* **407:** 98–102

Mignot T, Merlie JP, Zusman DR (2005) Regulated pole-to-pole oscillations of a bacterial gliding motility protein. *Science* **310:** 855–857

Mignot T, Shaevitz JW, Hartzell PL, Zusman DR (2007) Evidence that focal adhesion complexes power bacterial gliding motility. *Science* **315:** 853–856

Mittal R, Ahmadian MR, Goody RS, Wittinghofer A (1996) Formation of a transition-state analog of the Ras GTPase reaction by Ras-GDP, tetrafluoroaluminate, and GTPase-activating proteins. *Science* **273:** 115–117

Murshudov GN, Vagin AA, Dodson EJ (1997) Refinement of macromolecular structures by the maximum-likelihood method. *Acta Crystallogr D Biol Crystallogr* **53:** 240–255

Pasqualato S, Renault L, Cherfils J (2002) Arf, Arl, Arp and Sar proteins: a family of GTP-binding proteins with a structural device for 'front-back' communication. *EMBO Rep* **3:** 1035–1041

Patryn J, Allen K, Dziewanowska K, Otto R, Hartzell PL (2010) Localization of MglA, an essential gliding motility protein in Myxococcus xanthus. *Cytoskeleton* **67:** 322–337

Rensland H, John J, Linke R, Simon I, Schlichting I, Wittinghofer A, Goody RS (1995) Substrate and product structural requirements for binding of nucleotides to H-ras p21: the mechanism of discrimination between guanosine and adenosine nucleotides. *Biochemistry* **34:** 593–599

Sancak Y, Bar-Peled L, Zoncu R, Markhard AL, Nada S, Sabatini DM (2010) Ragulator-Rag complex targets mTORC1 to the lysosomal surface and is necessary for its activation by amino acids. *Cell* **141:** 290–303

Schaefer A, Höhner K, Berken A, Wittinghofer A (2011) The unique plant RhoGAPs are dimeric and contain a CRIB motif required for affinity and specificity towards cognate small G proteins. *Biopolymers* **95:** 420–433

Scheffzek K, Ahmadian MR (2005) GTPase activating proteins: structural and functional insights 18 years after discovery. *Cell Mol Life Sci* **62:** 3014–3038

Scheffzek K, Ahmadian MR, Kabsch W, Wiesmüller L, Lautwein A, Schmitz F, Wittinghofer A (1997a) The Ras-RasGAP complex: structural basis for GTPase activation and its loss in oncogenic Ras mutants. *Science* **277:** 333–338

Scheffzek K, Lautwein A, Scherer A, Franken S, Wittinghofer A (1997b) Crystallization and preliminary X-ray crystallographic study of the Ras-GTPase-activating domain of human p120GAP. *Proteins* **27:** 315–318

Scrima A, Thomas C, Deaconescu D, Wittinghofer A (2008) The Rap-RapGAP complex: GTP hydrolysis without catalytic glutamine and arginine residues. *EMBO J* **27:** 1145–1153

Shapiro L, McAdams HH, Losick R (2009) Why and how bacteria localize proteins. *Science* **326:** 1225–1228

Skerker JM, Berg HC (2001) Direct observation of extension and retraction of type IV pili. *PNAS* **98:** 6901–6904

Song J, Tyler RC, Lee MS, Tyler EM, Markley JL (2005) Solution structure of isoform 1 of Roadblock/LC7, a light chain in the dynein complex. *J Mol Biol* **354:** 1043–1051

Spoerner M, Herrmann C, Vetter IR, Kalbitzer HR, Wittinghofer A (2001) Dynamic properties of the Ras switch I region and its importance for binding to effectors. *PNAS* **98:** 4944–4949

Sprang SR (1997) G protein mechanisms: insights from structural analysis. *Annu Rev Biochem* **66:** 639–678

Sprang SR, Chen Z, Du X (2007) Mechanisms and pathways of heterotrimeric G protein signaling. *Adv Protein Chem* **74:** 1–65

Srinivasa SP, Watson N, Overton MC, Blumer KJ (1998) Mechanism of RGS4, a GTPase-activating protein for G protein alpha subunits. *J Biol Chem* **273:** 1529–1533

Sun H, Zusman DR, Shi W (2000) Type IV pilus of Myxococcus xanthus is a motility apparatus controlled by the frz chemosensory system. *Curr Biol* **10:** 1143–1146

Tee AR, Manning BD, Roux PP, Cantley LC, Blenis J (2003) Tuberous sclerosis complex gene products, Tuberin and Hamartin, control mTOR signaling by acting as a GTPase-activating protein complex toward Rheb. *Curr Biol* **13:** 1259–1268

Terwilliger TC (2002) Automated structure solution, density modification and model building. *Acta Crystallogr D Biol Crystallogr* **58:** 1937–1940

Tesmer JJ, Berman DM, Gilman AG, Sprang SR (1997) Structure of RGS4 bound to AlF4–activated G(i alpha1): stabilization of the transition state for GTP hydrolysis. *Cell* **89:** 251–261

Veltel S, Gasper R, Eisenacher E, Wittinghofer A (2008a) The retinitis pigmentosa 2 gene product is a GTPase-activating protein for Arf-like 3. *Nat Struct Mol Biol* **15:** 373–380

Veltel S, Kravchenko A, Ismail S, Wittinghofer A (2008b) Specificity of Arl2/Arl3 signaling is mediated by a ternary Arl3-effector-GAP complex. *FEBS Lett* **582:** 2501–2507

Vetter IR, Nowak C, Nishimoto T, Kuhlmann J, Wittinghofer A (1999) Structure of a Ran-binding domain complexed with Ran bound to a GTP analogue: implications for nuclear transport. *Nature* **398:** 39–46

Vetter IR, Wittinghofer A (2001) The guanine nucleotide-binding switch in three dimensions. *Science* **294:** 1299–1304

Wittinghofer A, Nassar N (1996) How Ras-related proteins talk to their effectors. *Trends Biochem Sci* **21:** 488–491

Wittinghofer A, Vetter IR (2010) Structure-function relationships of the G domain, a canonical switch motif. *Annu Rev Biochem* **80:** 943–971

Zhang Y, Franco M, Ducret A, Mignot T (2010) A bacterial Ras-like small GTP-binding protein and its cognate GAP establish a dynamic spatial polarity axis to control directed motility. *PLoS Biol* **8:** e1000430

Zurita-Martinez SA, Puria R, Pan X, Boeke JD, Cardenas ME (2007) Efficient Tor signaling requires a functional class C Vps protein complex in Saccharomyces cerevisiae. *Genetics* **176:** 2139–2150